UCLA

Title

Seismic earth pressures exerted on rigid walls by vertically heterogeneous soil using Winkler method

Permalink

https://escholarship.org/uc/item/2zk3c2d6

Authors

Brandenberg, SJ

Agapaki, E

Mylonakis, G

et al.

Publication Date

2023-12-11

Peer reviewed

SEISMIC EARTH PRESSURES EXERTED ON RIGID WALLS BY VERTICALLY HETEROGENEOUS SOIL USING WINKLER METHOD

S.J. Brandenberg[1], E. Agapaki[2], G. Mylonakis[3], and J.P. Stewart[4]

[1] *Associate Professor, Department of Civil and Environmental Engineering, UCLA, sjbrandenberg@ucla.edu*
[2] *Graduate Student Researcher, Department of Civil and Environmental Engineering, UCLA, agapakieva@gmail.com*
[3] *Professor, Department of Civil Engineering, University of Bristol, g.mylonakis@bristol.ac.uk*
[4] *Professor and Chair, Department of Civil and Environmental Engineering, UCLA, jpstewart@seas.ucla.edu*

Abstract

During earthquake ground shaking earth pressures on retaining structures can cyclically increase and decrease as a result of inertial forces applied to the walls and kinematic interactions between the stiff wall elements and surrounding soil. Limit equilibrium analysis imposes a pseudo-static inertial force to a soil wedge behind the wall (the mechanism behind the widely-used Mononobe-Okabe method), which is a poor analogy for either inertial or kinematic wall-soil interaction. Many basement walls and retaining structures are dominated by kinematic soil-structure interaction (SSI) effects arising from differences in displacement between the wall and the free-field soil. Kinematic SSI solutions are often formulated for uniform soil conditions, but the shear modulus of most soils is known to increase with mean effective stress, and therefore with depth. We examine the influence of vertical heterogeneity of shear modulus on kinematic SSI for rigid walls. An existing free-field displacement solution is presented first, followed by analysis of earth pressure increments using a Winkler assumption. Vertical heterogeneity is shown to reduce seismic earth pressures compared with a uniform soil case (for a given frequency and peak ground surface displacement) because free-field displacements are largest near the surface, where the soil is softest and Winkler stiffness is lowest. The proposed Winkler solution is then compared with an exact analytical solution for vertically heterogeneous soil over a rigid base and retained between two opposing rigid walls. The agreement is imperfect, but reasonable, with differences likely due to assumptions regarding the dynamic Winkler stiffness intensity.

Keywords: soil-structure interaction, retaining walls, seismic earth pressure, Winkler

1. Introduction

The increment of lateral earth pressure that should be applied to a retaining wall to account for earthquake effects is currently a source of confusion among design professionals. Current guidelines documents (e.g., NCHRP 2008) utilize a limit equilibrium analysis in which a pseudo-static coefficient acts upon an active Coulomb-type wedge in frictional soil. Based on the classical work of Okabe [2] and Mononobe and Matsuo [3], this approach is widely known as the Mononobe-Okabe (M-O) method. Variants of the M-O method have been proposed by [4], [5], [6], [7] and [8], all of which are rooted in the limit equilibrium analysis framework.

Recent experimental research has challenged the M-O method as being overly conservative (e.g., [9], [10]), while elastodynamic solutions have found seismic earth pressures may significantly exceed those prescribed by the M-O method (e.g., [11], [13], [12], [17], [18], [20]). These conflicting findings have driven much of the confusion among the engineering community regarding seismic earth pressures. A fundamental problem with the M-O method is that it does not adequately reflect the manner in which vibrating soil interacts with a retaining structure. Though the elastodynamic solutions are better equipped to capture this interaction, they are often formulated for conditions where a rigid base underlies an elastic soil layer being retained by a rigid wall over its full thickness (i.e., a "bathtub" condition). These boundary conditions result in significant amplification at the resonant modes of the soil column, which in turn produce large relative wall-soil displacements and seismic earth pressures.

A kinematic soil-structure interaction solution developed by [14] demonstrates that kinematic seismic earth pressures are fundamentally controlled by relative wall-soil displacements, which in turn are controlled by the ratio of the wavelength of the vibrating free-field soil column, λ, to the height of the wall, H. When λ/H is large, the free-field shear strain acting along the wall height is small, the wall and free-field soil move nearly in tandem, and the kinematic earth pressures are also small. Walls resting on thick soil layers excited by earthquake ground motions typically exhibit large λ/H ratios, resulting in small earth pressures. This was the condition in the recent experimental studies for which smaller-than-M-O pressures were measured. Conversely, the bathtub condition results in significant energy at the first mode frequency of the soil column (which occurs at $\lambda/H = 4$ for uniform elastic soil), generating large, greater-than-M-O, seismic earth pressures. The kinematic framework presented by [14] explains both the experimental observations and elastodynamic solutions in a single framework.

A number of simplifying assumptions were made in deriving the kinematic solution for seismic earth pressures by [14]. First, the soil was modeled as an isotropic elastic homogeneous material. The shear modulus of soil is known to vary with effective confining pressure, therefore this assumption is generally not representative of typical soil profiles. Second, the wall was modeled as rigid, whereas basement walls and free-standing retaining walls may have sufficient flexibility to influence mobilized earth pressures. Third, soil inelasticity was not modeled explicitly, though strain-compatible moduli can be selected to render the method equivalent-linear. Finally, gapping and shear slip at the soil-wall interface was not modeled. The focus of this paper is to explore the influence of vertical heterogeneity of the shear modulus on the mobilization of seismic earth pressures. To facilitate comparisons to exact analytical solutions in the literature ([17], [18]) solutions are developed herein for rigid walls fixed to a rigid base layer (e.g., the bathtub condition), though the solution framework for handling vertical heterogeneity is easily adaptable to deeper soil conditions. The framework for computing free-field displacements and seismic earth pressures is presented first, followed by comparison with an exact analytical solution. Elastodynamic solutions for flexible walls, soil inelasticity, gapping, and interface slip is reserved for future publications.

2. Solution for Free-Field Displacement in Vertically Heterogeneous Soil

An analytical solution for vertical shear waves propagating through a soil layer with V_S varying vertically in accordance with Eq. 1 was developed by [15], where V_H is the shear wave velocity at the bottom of the layer (depth = H), V_o is the shear wave velocity at the ground surface, z is depth, and n is an exponent controlling the rate of change of V_S with depth. Solutions were developed for the vertically heterogeneous layer resting on a

rigid base, and for a vertically heterogeneous layer resting on a uniform elastic layer on a rigid base. The former solutions are utilized herein.

$$V_s = V_H \left[b + (1 - b) \frac{z}{H} \right]^n$$

$$b = \left(\frac{V_o}{V_H} \right)^{1/n}$$

(1)

The analytical solution for the free-field soil displacement, u_{ff}, is given by Eq. 2, where $J_{v2}()$ and $N_{v2}()$ denote Bessel functions of the first and second kind, respectively, of order $v2$. Note that V_r is the shear wave velocity at a reference depth, z_r. For simplicity, z_r can be set equal to H, in which case $V_r = V_H$.

$$u_{ff}(z) = \frac{C_1 \left(b + q \frac{z}{z_r} \right)^m}{N_{v2+1}\left(\lambda b^{1/2} \right)} \left\{ J_{v2} \left[\lambda \left(b + q \frac{z}{z_r} \right)^{1/2} \right] N_{v2+1}\left(\lambda b^{1/2} \right) - J_{v2+1}\left(\lambda b^{1/2} \right) N_{v2} \left[\lambda \left(b + q \frac{z}{z_r} \right)^{1/2} \right] \right\}$$

$$\lambda = 2(1 - n)$$

$$m = (1 - 2n)/2$$

$$n2 = (2n - 1)/2(1 - n)$$

$$\lambda = 2k_r z_r / \lambda q$$

$$q = 1 - b$$

$$k_r = w / V_r$$

(2)

The modal frequencies are obtained by solving the characteristic equation (Eq. 3), where m=0,1,2… corresponds to the different modes. The roots of Eq. 3 correspond to the modal frequencies, and require solution of λ_m and subsequently substituting λ_m into Eq. (4).

$$J_{v2+1}\left(\lambda_m b^{1/2} \right) N_{v2} \left(\lambda_m \right) - J_{v2}\left(\lambda_m \right) N_{v2+1}\left(\lambda_m b^{1/2} \right) = 0$$

(3)

$$f_m = \frac{V_H}{2pH}(1 - n)(1 - b)\lambda_m$$

(4)

Fig. 1 illustrates five velocity profiles corresponding to a vertically heterogeneous layer resting on a rigid base for various values of n, and for $b = 0.01$. The value of V_H was selected such that the time-averaged shear wave velocity, $V_{S,av}$ is constant for all five profiles, as illustrated using Eq. (5). The first-mode frequency of a soil layer is often computed as $f_0 \approx V_{S,av}/4H$, which is not analytically rigorous but provides a reasonable approximation in many cases, and avoids the complexity of finding the roots of Eq. 3. For the case shown in Fig. 1, the ratio $f_0/(V_{S,av}/4H) = (1.0, 1.047, 1.089, 1.086, 0.987, 0.847)$ for $n = (0.0, 0.1, 0.25, 0.5, 0.75, 0.9)$. The average shear wave velocity for this profile is defined as:

$$V_{s,av} = \frac{H}{\displaystyle\int_0^H \frac{dz}{V_s(z)}} = \frac{H}{\displaystyle\int_0^H \frac{dz}{V_H \left[b + (1-b)\dfrac{z}{H} \right]^n}} = \frac{V_H (1-b)(1-n)}{1 - b^{1-n}} \tag{5}$$

The first mode shapes depend significantly on n. The first mode shape with $n=0.1$ is approximately equal to the first mode shape for a uniform layer ($n=0$) with shear strains being largest near the base of the layer, while the mode shape for $n=0.5$ is nearly linear with shear strains being approximately constant, and the mode shape for $n=0.9$ exhibits small displacements near the base and the highest strains at shallow depths ([19]).
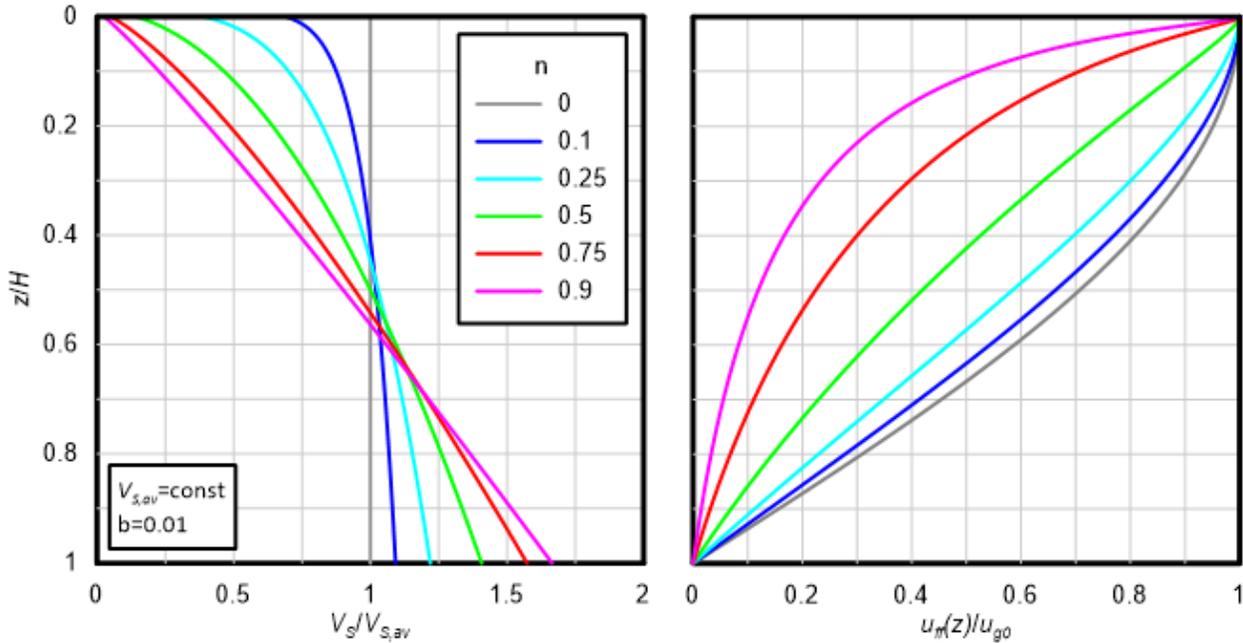
Fig. 1 – Normalized shear wave velocity and first-mode displacement for vertically heterogeneous layer resting atop a rigid base. All profiles have a constant $V_{S,av}$ (after [15]).

3. Winkler Stiffness Intensity Approximation

The lateral stiffness associated with wall-soil interaction is represented by stiffness intensity k_y^i, which has units of stiffness/area. The solution for kinematic seismic earth pressures by [14] requires the use of expressions for k_y^i, which was uniform with depth due to the homogeneous soil assumption.

For the present application, we use an approximate k_y^i solution from [16]. This solution applies for a rigid wall of height H resting on a rigid base and supporting uniform elastic soil subjected to excitation from the base. The derived solution for k_y^i is frequency-dependent, which is expressed as a function of the dimensionless frequency, $a_o = \omega H/V_S^*$, and a dimensionless cutoff frequency, a_{oc}, which is equal to $\pi/2$ for the harmonic shape functions adopted by [16]. Note that $V_S^* = V_S \cdot (1+2iD)^{0.5}$ is the complex shear wave velocity incorporating the effects of frequency-independent material damping D. Because V_S^* varies with depth, a representative value of $V_S^* = (4Hf_n)$ was selected for computing a_o, where f_n is the first-mode frequency computed using Eq. (4). This value was selected because a uniform soil profile with V_S^* would produce the same first mode frequency as the vertically heterogeneous profile. To account for vertical heterogeneity in the stiffness intensity term, we adjust the form proposed by [16] such that k_y^i is a function of depth, and is directly proportional to $G(z) = \rho V_S(z)^2$, where ρ is

mass density and *G* is shear modulus. Though this approximation is not analytically rigorous, an alternative relationship is not currently available for heterogeneous soil profiles. The assumed relation for $k_y^i(z)$ is given by Eq. 7, where □ is the Poisson ratio.

$$k_y^i\left(z\right) = \frac{r\,V_s(z)^2}{H}\,\frac{p}{\sqrt{\left(1-n\right)\left(2-n\right)}}\,\sqrt{a_{oc}^2 - a_o^2}\left(1+2iD\right) \tag{7}$$

An average value of Winkler stiffness intensity, $k_{y\,av}^i$ is obtained by substituting $V_{S,av}$ for $V_S(z)$ in Eq. (7).

4. Example Kinematic SSI Solutions

Example solutions are presented in this section for the seismic earth pressure imposed on a rigid wall by a vertically heterogeneous profile. Various values of the vertical heterogeneity exponent, *n*, are used to illustrate its influence on seismic earth pressure. The seismic earth pressure increment is computed using Eq. (8), while the resultant, P_E, is computed using Eq. (9) and the normalized height of the resultant, *h/H*, is computed using Eq. (10).

$$\Delta s_h\left(z\right) = u_{ff}(z)\,k_y^i(z) \tag{8}$$

$$P_E = \int_0^H u_{ff}(z)\,k_y^i(z)\,dz \tag{9}$$

$$\frac{h}{H} = \frac{\int_0^H z\,u_{ff}(z)\,k_y^i(z)\,dz}{P_E} \tag{10}$$

Pressure distributions are presented in Fig. 2 in terms of the horizontal seismic pressure increment, □□$_{yy}$ normalized by $k_{y\,av}^i u_{g0}$ associated with the first-mode resonant frequency of the free-field soil column. As *n* increases, the seismic earth pressures decrease significantly, particularly at shallow depths, and the centroid of the resultant force shifts downward. These differences are attributed to the mode shapes combined with the depth-variation in k_y^i. For high *n* values, the mode shapes in Figure 1 show that free-field displacements are small near the base of the profile, where k_y^i is large, and large near the surface of the profile where k_y^i is small.
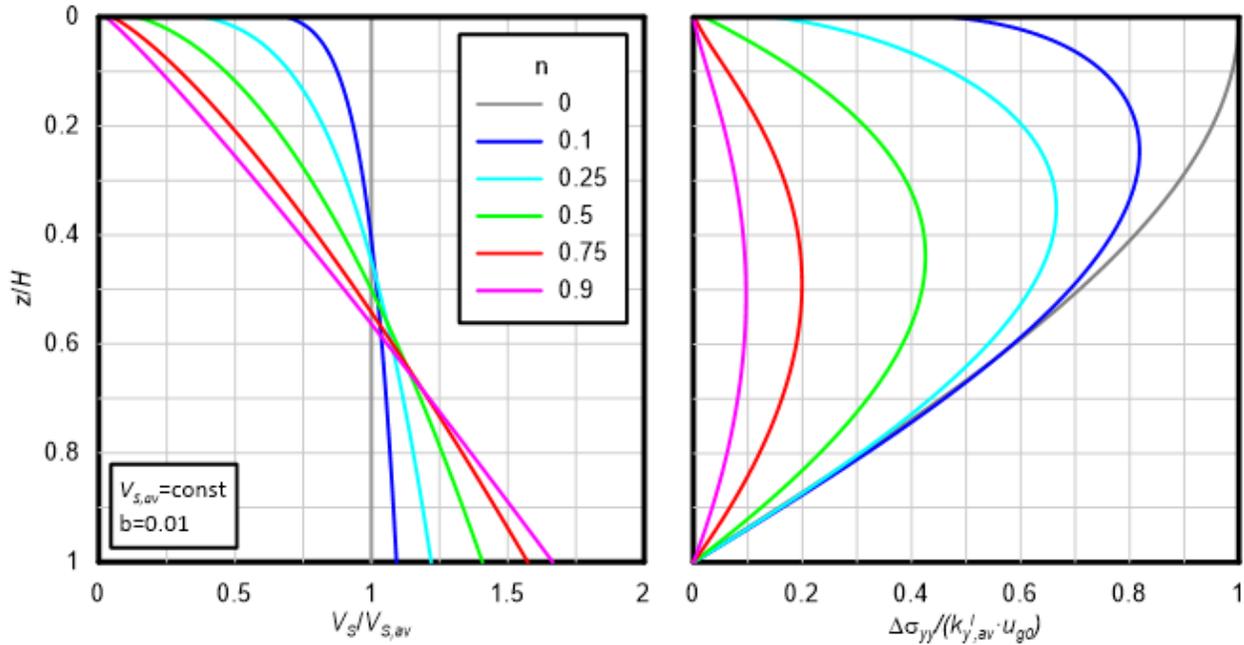
Fig. 2 – Dimensionless horizontal seismic earth pressure increment versus dimensionless depth for vertically heterogeneous soil profiles acting against a rigid vertical wall.

Transfer functions relating the amplitude of the dimensionless seismic earth pressure resultant, P_E, to λ_{av}/H are shown in Fig. 3, where $\lambda_{av} = V_{S,av}/f$. As n increases, the rightmost peak of the transfer functions decreases significantly in amplitude, as anticipated by the reductions in earth pressures over the upper portion of the wall shown in Fig. 2. Furthermore, the peak shifts to larger λ_{av}/H. The shift in the position of the peak is related to the distribution of free-field shear strain over H.

We recognize that the results in Figure 3 use a time-averaged shear wave velocity, $V_{S,av}$ that provides only an approximation of the modal response of the soil column. Errors associated with this approximation transfer to the normalizing factors λ_{av} and $k_y^i{}_{av}$. The approximation is utilized herein for simplicity since $V_{S,av}$, λ_{av}, and $k_y^i{}_{av}$ can easily be computed.

Also plotted in Fig. 3 is the normalized depth of the resultant, h/H. As n increases, the h/H decreases at wavelengths longer than the right-most peak. The resultant position at low λ_{av}/H values varies rapidly with changes in λ_{av}/H due to the fluctuations of seismic pressure over the wall height, and the resultant is not constrained to act in the interval from 0 to H. For example, at certain frequencies $P_E = 0$, but the resulting pressure distribution produces a non-zero moment, M_E, about the base of the wall. Since $h = M_E/P_E$, h becomes infinite. The notion of a resultant height is not physically meaningful in these cases.
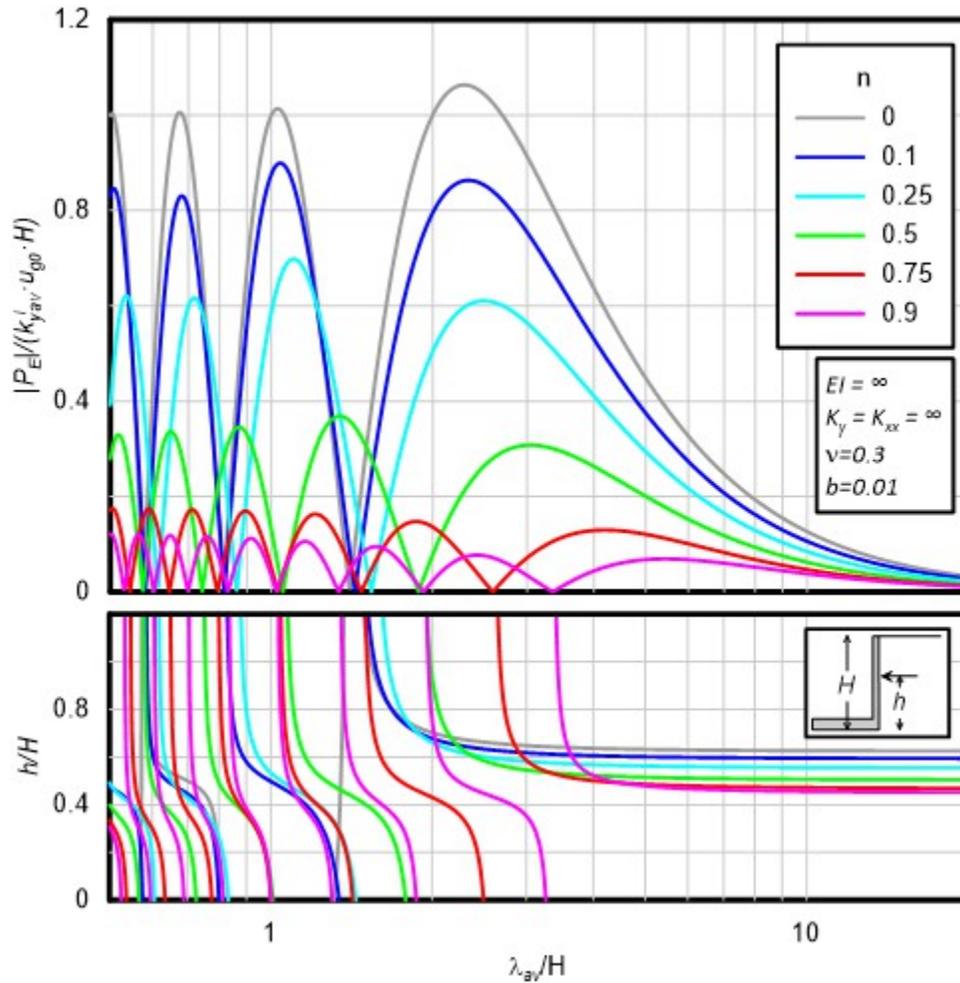
Fig. 3 – Normalized seismic earth pressure resultant and height of resultant versus normalized wavelength for vertically heterogeneous soil profiles acting on a rigid wall.

5. Comparison With Exact Analytical Solution

The proposed solutions are approximate in several respects. First, they utilize the Winkler assumption, which is an approximation that is commonly applied in cases where complicated boundary conditions render rigorous analytical solutions infeasible. Second, the Winkler stiffness intensity, k_y^i, was assumed to be proportional to shear modulus, and the solution by [16] was adapted to this assumption.

To validate the results obtained using the proposed simplified framework, we compare our findings to exact analytical solutions developed by [18] for the seismic earth pressures imposed on rigid walls resting on a rigid base retaining vertically heterogeneous soil. The analytical solution is formulated for a symmetric condition in which soil is retained between two walls of height H separated by distance L. The largest ratio they studied was $L/H = 10$, which is adopted for comparison herein because it corresponds most closely to a single wall condition. The vertical variation of shear modulus is defined by Eq. (11), where G_o is the shear modulus at the ground surface, G_∞ is the shear modulus at a depth of infinity, and ⧠ is a constant that controls the rate of change of shear modulus with depth. Mass density ⧠ was assumed as depth-invariant in their solution.

$$G(z) = G_o + \left(G_\infty - G_o\right)\left(1 - e^{-h\frac{z}{H}}\right) \tag{11}$$

The shear modulus corresponding to Eq. (1) and Eq. (11) are different, and we seek to fit Eq. (1) to best fit Eq. (11). To achieve this goal, a dimensionless shear wave velocity profile was computed by taking the square root of Eq. (11), and normalizing by the value of the resulting expression at $z = H$. Normalized velocity profiles are shown in Fig. 4 for various values of $\chi = 1 - G_o/G_\infty$. The constants in Eq. (1) were then fit to these normalized velocity profiles by dividing Eq. (1) by V_H, setting V_o/V_H to be equal to the values at $z=0$ implied by Eq. 11, and solving for n such that the time-averaged normalized shear wave velocity profiles were equal.
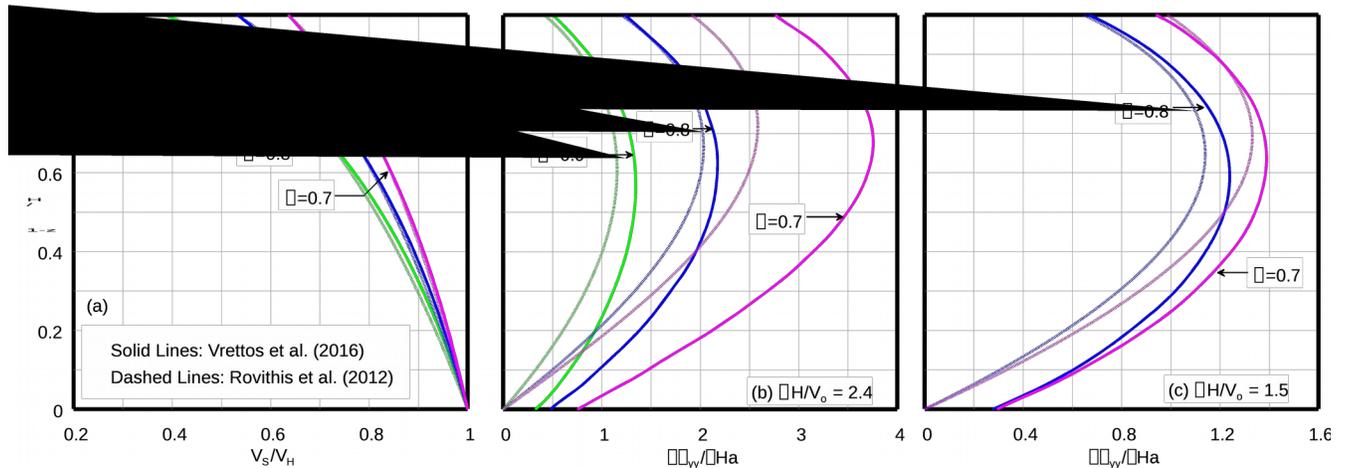
Fig. 4 – (a) Normalized shear wave velocity profiles, and normalized seismic earth pressures versus normalized depth for the analytical solution by [18] compared with the proposed solution. Solutions are for (b) $\omega H/V_o = 2.4$, (c) $\omega H/V_o = 1.5$, $\chi = 0.3$, and $\zeta = 0.05$.

Normalized seismic earth pressures presented by [18] are compared with those implied by the solution for free-field displacements by [15] multiplied by the Winkler stiffness intensity in Eq. (7). These solutions are presented for two different dimensionless frequencies of (b) $\omega H/V_o = 2.4$ and (c) $\omega H/V_o = 1.5$. For (b), the proposed solution modestly under-predicts seismic pressures for $\chi = 0.9$ and 0.8, and more significantly under-predicts for $\chi = 0.7$. For (c) the proposed solution slightly under-predicts seismic pressures. A number of factors may be at work in explaining the under-prediction. First, the solutions for (b) are all fairly close to first-mode resonance ($\omega/\omega_o = 0.68$, 0.9, and 1.06 for $\chi = 0.9$, 0.8, and 0.7, respectively). The stiffness modifier term in Eq. (7) [i.e., $(a_{oc}^2 - a_o^2)^{0.5}$] is a significant contributor to the values of k_y^i when the frequency is near a resonant mode, but there is considerable uncertainty in applying a stiffness modifier term formulated for homogeneous soil to a heterogeneous profile. The amplitude of the error is expected to increase as ω/ω_o becomes closer to unity. The agreement is much better at lower frequencies where the stiffness modifier is less important. Another possible cause of the difference is that the first-mode frequencies of the two soil profiles are likely slightly different due to the misfit in the V_s/V_H profiles in Fig. 4. Solutions for σ_{yy} are very sensitive to small changes in frequency when ω/ω_o is near unity, hence a small difference in ω_o could translate to a significant difference in σ_{yy}. Furthermore, the solution by [18] corresponds to a two-dimensional problem with soil contained between two walls, while the natural frequency for the proposed solution corresponds to 1-D free-field response. Despite these differences, the proposed method provides a reasonable agreement with the [18] analytical solutions.

The proposed solutions result in zero seismic earth pressure at the base of the wall because there is zero relative displacement at this position, as required in a Winkler-type solution by the rigid base assumption . However, the analytical solutions do predict some seismic pressure at this depth. This illustrates a fundamental limitation of

the Winkler solution that causes an under-prediction of seismic earth pressure, and an over-prediction of the height of the resultant force.

Although not shown in this paper, the proposed method is adaptable to walls resting on deep soil profiles, which is a more common boundary condition than the rigid base condition. Seismic earth pressures reduce significantly for such flexible-based conditions as compared to rigid base conditions because the wall is better able to conform to the free-field displacement profile, and the wavelengths controlling seismic excitation tend to be longer.

6. Conclusions

Vertical heterogeneity in which the free-field shear wave velocity profile increases with depth causes decreases in kinematic earth pressures on rigid walls during seismic shaking, relative to the uniform soil condition, for a constant ground surface motion amplitude. The cause of the reduction is that free-field displacements become concentrated near the ground surface as the degree of heterogeneity increases, where the Winkler stiffness intensity is small. More than an order of magnitude reduction in the peak response is predicted as n transitions from 0 (uniform V_S profile) to 1 (linear V_S profile). Furthermore, the height of the resultant of the seismic earth pressure distribution shifts downward as a result of vertical heterogeneity from h/H larger than 0.6 for uniform soil to slightly more than 0.4 for linearly increasing V_S.

The proposed Winkler solution combined with the [15] free-field displacement solution agreed reasonably well with the exact analytical solution developed by [18]. The former under-predicted the earth pressures computed by the latter, with the likely cause of the difference being the selection of dynamic Winkler stiffness intensity. The [18] solutions used for comparison herein were fairly close to the resonant frequency of the free-field soil column, and frequency modifiers to the stiffness terms are known to be important near resonance. Future research regarding appropriate selection of Winkler stiffness intensity has the potential to improve the agreement.

Wall flexibility, base stiffness, soil inelasticity, gapping, and interface slip are all known contributors to seismic earth pressures. The influence of these effects is beyond the scope of this study, and is reserved for future publications.

7. Acknowledgments

8. References

[1] NCHRP (National Cooperative Highway Research Program). (2008). "Seismic analysis and design of retaining walls, buried structures, slopes, and embankments." *Rep. 611*, D. G. Anderson, G. R. Martin, I. P. Lam, and J. N. Wang, eds., National Academies, Washington D.C.

[2] Okabe, S. (1924). "General theory of earth pressure and seismic stability of retaining wall and dam." *Journal of Japan Society of Civil Engineers,* 12(4):34-41.

[3] Mononobe, N., and Matsuo, M. (1929). "On the determination of earth pressures during earthquakes." *Proc. World Engineering Congress*, Engineering Society of Japan, Tokyo, 179-187.

[4] Seed, H.B., and Whitman, R.V. (1970). "Design of earth retaining structures for dynamic loads." *Proc., ASCE Specialty Conf. on Lateral Stresses in the Ground and Design of Earth Retaining Structures*, Vol. 1, Reston, VA, 103-147.

[5] Chen, W. F. (1975). "Limit analysis and soil plasticity. Developments in geotechnical engineering", *Elsevier*, Amsterdam, Netherlands.

[6] Chen, W. F., and Liu, X. L. (1990). "Limit analysis in soil mechanics", *Elsevier*, Amsterdam, Netherlands.

[7] Steedman, R. S., and Zeng, S. (1990). "The influence of phase on the calculation of pseudo-static earth pressure on a retaining wall." *Geotechnique*, 40(1):103-112.

[8] Mylonakis, G, P Kloukinas, and C Papantonopoulos, (2007). "An alternative to the Mononobe–Okabe equations for seismic earth pressures", *Soil Dynamics and Earthquake Engineering*, 27:957-969.

[9] Al Atik, L. and Sitar, N. (2010). "Seismic earth pressures on cantilever retaining structures." *Journal of Geotechnical and Geoenvironmental Engineering*, 10.1061/(ASCE)GT.1943-5606.0000351, 1324-1333.

[10] Lew, M., Sitar, N., and Al-Atik, L. (2010). "Seismic earth pressures: Fact or fiction?" *Proc., Earth Retention Conf.*, R. Finno, Y. M. A. Hashash and P. Arduino, eds., ASCE, Reston, VA.

[11] Wood, J. H. (1973). "Earthquake induced soil pressures on structures." *Rep. No. Earthquake Engineering Research Laboratory (EERL) 73-05*, California Institute of Technology, Pasadena, CA.

[12] Ostadan, F. (2005). "Seismic soil pressure for building walls—An updated approach." *Soil Dynamics and Earthquake Engineering*, 25(7-10), 785-793.

[13] Veletsos, A.S. and Younan, A.H. (1994). "Dynamic Soil Pressures on Rigid Vertical Walls", *International Journal of Earthquake Engineering and Structural Dynamics*, 23:275-301.

[14] Brandenberg, S.J., Mylonakis, G., and Stewart, J.P. (2015). "Kinematic framework for evaluating seismic earth pressures on retaining walls." *Journal of Geotechnical and Geoenvironmental Engineering*, 1090-0241/04015031.

[15] Rovithis, E.N., Parashakis, H., and Mylonakis, G.E. (2011). "1D harmonic response of layered inhomogeneous soil: Analytical investigation." *Soil Dynamics and Earthquake Engineering*, 31, 879-890.

[16] Kloukinas, P., Langoussis, M., and Mylonakis, G. (2012). "Simple wave solution for seismic earth pressures on non-yielding walls." *Journal of Geotechnical and Geoenvironmental Engineering*, 10.1061/(ASCE)GT.1943-5606.0000721, 1514-1519.

[17] Papagiannopoulos GA, Beskos D.E., Triantafyllidis T. (2015). "Seismic pressures on rigid cantilever walls retaining poroelastic soil: An exact solution", *Soil Dynamics and Earthquake Engineering*, 77:208-219.

[18] Vrettos C., Beskos D.E., Triantafyllidis T., (2016). "Seismic earth pressures on rigid cantilever walls retaining elastic continuously non-homogeneous soil: An exact solution", *Soil Dynamics and Earthquake Engineering*, 82:142-153.

[19] Mylonakis G.E., Rovithis E.N., Parashakis H. (2013). "1D Harminic Response of Layered Inhomogeneous Soil: Exact and Approximate Analytical Solutions", Computational Methods in Earthquake Engineering, Springer, 2:1-32.

[20] Wu G., Finn WDL. (1999). "Seismic lateral pressures for design of rigid walls". Canadian Geotechnical Journal, 36:509-522.